Estimation of extreme precipitations in Estonia and Italy using dual-pol weather radar QPEs

R. Roberto Cremonini [*1,3], T. Tanel Voormansik[2,4], P. Piia Post[2], and D. Dmitri Moisseev[3,5]

[1]Department of Physics, University of Helsinki, Finland
[2]Institute of Physics, University of Tartu, Estonia
[3]Regional Agency for Environmental Protection of Piemonte, Department for Natural and Environmental Risks, Torino, Italy
[4]Estonian Environment Agency, Tallinn, Estonia
[5]Finnish Meteorological Institute, Helsinki, Finland

Correspondence: Roberto Cremonini (rcremoni@ad.helsinki.fi)

Abstract. Climatology of Evaluating extreme rainfalls for a certain location is commonly taken into account designing storm water considered when designing stormwater management systems. Rain gauge data have often been are widely used to estimate rainfall intensity intensities for a given return period. However, the poor spatial and temporal resolution of operational gauges networks is the main limiting factor. Several studies have used rainfall estimates based on weather radar horizontal reflectivity (Z_h), but they come with a great caveat: while proven reliable on low or moderate rainfall rates, they are subject to major errors in extreme rainfall and convective cases. In fact, it It is widely known that C-band weather radar can both underestimate precipitation intensity due to signal attenuation or overestimate it due to hail contamination. and clutter contamination. Since the late 1990s dual-polarization weather radar started to become operational in the National Surveillance radar network in Europe, providing innovative QPE estimation based on polarimetric variables. This study circumvents these Z_h shortcomings by using specific differential phase (K_{dp}) data from dual polarization operational dual-polarization C-band weather radarswhich . The rain intensity estimates based on specific differential phase are immune to attenuation and hail contamination issuesless affected by hail contamination.

The aim of this study is to estimate depth-duration-frequency (DDF) curves from This preliminary study aims to estimate return periods for 1-hour rainfall total computed using polarimetric weather radar data using quantitative precipitation estimations (QPEs) based on K_{dp} $R(Z_h, K_{dp})$ data and to compare results with raingauges derived ones. Single the results with those ones derived using $R(Z_h)$ and rain-gauge data. Only the warm period during the year is here considered, as most of the extreme precipitation events for such duration take place for both places at this time. Limiting the dataset to warm period also allows us to use the radar-based rainfall quantitative precipitation estimates, which are more reliable than the snowfall ones. Data from operational dual polarimetric C-band weather radar site data sites are used both from Estonia and Italy . From Italy radar data, available with five minutes temporal resolution and from years 2012-2020, from Bric della Croce dual-polarization Doppler C-band radar located in Turin, Northern Italy are used. The Estonian Environment Agency operates Sürgavere dual-polarization Doppler C-band radar, located in central Estoniain Viljandi county; observations are available with

*Corresponding author: Roberto Cremonini, Department of Physics, University of Helsinki, Finland, e-mail: rcremoni@ad.helsinki.fi

15-minutes temporal resolution and from years 2010-2020. Lowest completely free level Plan Position Indicator (PPI) scans are used to derive weather radar QPEs based on Z_h andK_{dp}Italy and Estonia. The comparison of weather radar return period estimations with ones derived from longterm gauges observations showed a good agreementGiven climatological homogeneous regions, this study demonstrates that polarimetric weather radar observations can provide reliable QPEs compared to single polarization estimates respect to rain gauges and, that can provide a reliable estimation of return periods 1-hour rainfall total, even for relatively short time series.

1 Introduction

The increase in artificial surfaces , as urbanization grows, determines a corresponding impervious surfaces due to urbanization leads to increase in flooding frequency due to poor infiltration and faster concentration time. The hydrological changes, driven by heavy urbanization, and resulting impacts on extreme rainfall, are also being established: a significant amount of research over the last twenty years has shown a strong relationship between urban areas and local microclimate.

Moreover, as stated by IPCC Fifth Assessment Report (?), in the near future The IPCC Sixth Assessment Report (IPCC, 2021) increased the interest on short-duration rainfall extremes estimations as several Earth regions are likely to be affected by an increase in number of heavy precipitation events due to climate change (?)in the near future due to the global warming. In Europe Besselaar et al. (2012) demonstrated that higher latitudes are yet experiencing an increment in intensity and frequency of extreme events, and correspondingly in heavy precipitations. For all these reasons, studies on extreme annual rainfall maximum depths for short durations are extremely relevant for hydrological studies, water management, and urban areas development (Marra et al., 2017).

However, the reliability of traditional rainfall depths estimations are is often limited by the low spatial density of rain gauge networks, particularly for short durations (Overeem et al., 2010). Nevertheless, single polarization single-polarization weather radars can provide quantitative precipitation estimates (QPEs), based on $Z_h - R$ relationships , empirical relationships between the equivalent reflectivity factor at horizontal polarization (Z_h) and the rain rate with proper spatial and temporal resolution. Several studies investigated statistics of extreme areal rainfall depths obtained from single polarization weather radar (Frederick et al., 1977; Allen et al., 2005b; Overeem et al., 2008, 2009a, b, 2010; ?; Marra and Morin , 2015; Panziera et al., 2018) single-polarization weather radar (Frederick et al., 1977; Allen et al., 2005b; Overeem et al., 2008, 2009a, b, 2010; Marra and Morin , 201 . Keupp et al. (2017) and Fabry et al. (2017) offer a complete review of monthly or annual rainfall climatology based on weather radar observations respectively in Europe and in the CONUS the the contiguous United States (CONUS) area.

However, due to signal attenuation at C-band (Delrieu et al., 2000) and due to precipitation overestimation for hail contamination (Ryzhkov et al., 2013), the horizontal radar reflectivity (Z_h) is subjected to major errors, especially during intense rainfalls and convective precipitations. As stated by Fairman et al. (2015), relevant underestimations typically can be found in areas of high elevation, QPEs underestimations typically occurs in mountainous areas and far away from the radar, or both; beam blocking weather radar; beam-blocking and overshooting also cause large differences between radar-based QPEs and reference gauges. To overcome these limitations, several adjustment techniques have been developed, correct-

ing QPEs, derived from ~~single polarization~~ single-polarization weather radar, with raingauges measurements (Einfalt and Michaelides , 2008; Goudenhoofdt and Delobbe, 2009). ~~Studies like Overeem et al. (2009b) and ?~~ Overeem et al. (2009b) derived short-duration extreme rainfall depths from gauges-adjusted weather radar QPEs. ~~Bringi and Chandrasekhar (2001) and Ryzhkov et al. (2005)~~ Barndes et al. (2001), Ryzhkov et al. (2005) and Vulpiani et al. (2012) demonstrated that polarimetric rainfall estimation algorithms based on specific differential phase (K_{dp}) outperform the conventional QPEs based on horizontal radar reflectivity, being immune from partial beam-blocking, attenuation, hail contamination, and weather radar miscalibration. Several studies focused on the evaluation of $R(K_{dp})$ relationships performances with respect to traditional ~~$R(Z)$~~ $R(Z_h)$ for precipitation events (Paulitsch et al., 2009; Moisseev et al., 2010; Cremonini and Bechini, 2010). ~~?~~ Voormansik et al. (2021a) deeply analyzed five years QPEs derived from operational C-band polarimetric weather radar in Estonia and Italy, demonstrating that $R(Z_h, K_{dp})$ relationships provide good quality QPEs.

For the first time, this study investigates the statistical properties of annual rainfall maximum for ~~short-durations analysing~~ 1-hour rainfall total, analyzing QPEs derived from $R(Z_h, K_{dp})$ observations by operational ~~dual polarization~~ dual-polarization C-band weather radars in two different climate regions. The results derived from short period weather radar observations are compared with statistics obtained from gauges measurements and ~~from~~ QPEs based on traditional horizontal radar reflectivity. Section 2 provides a description of study areas, polarimetric weather radar systems, and algorithms used to derive QPEs. In Section 3 extreme value statistic is applied to derive ~~depth-duration-frequency (DDF) curves, which describe the~~ ti fit the parent distributions, providing rainfall depth as a function of duration for given return periods. Finally, discussion and conclusions follow.

2 Materials and methods

This study focuses on QPEs based on polarimetric C-band weather radar, operating in Northern Italy and ~~in~~ Estonia. The studied period is limited to the warm period of the year as most of the extreme precipitation events at short temporal scales take place at this time. Limiting the dataset to warm period also helps to exclude that weather radar observations come from snow or ice crystals, a requirement for reliable rainfall intensity estimations based on $R(Z_h, K_{dp})$.

2.1 The study areas

This study focuses on areas in Piemonte, Italy, and ~~in~~ Estonia, covered by operational ~~dual polarization~~ dual-polarization Doppler C-band weather radars operated by the local weather services.

Piemonte is located in ~~the~~ northwestern Italy, in the upper areas of the Po valley; the central part of the region is relatively flat (300-200 m a.s.l.) with the Torino hill that reaches 770 meters a.s.l.. The Alps surround plains with altitudes ranging from 1,000 m to more than 4,500 m a.s.l.. The two areas considered in this study are centered on Torino hill and they extend for about ~~40~~ 30-50 km far from the weather radar, corresponding to about 7,300 km^2 altogether (Figure ~~??~~1, the left map). To ensure QPEs data quality, the choice to restrict the study areas close to the radar site is driven by these main reasons:

1. to reduce weather radar beam-broadening and ~~beam propagation~~ beam-propagation effects;

2. to avoid the Alps complex orography in western and northern ~~direction~~directions;

3. to limit the weather radar beam height above ground;

4. to avoid or to limit spatial non-stationarity of the GEV parameters and their dependence from geomorphology (altitude, terrain slope and exposition).

The Piemonte rainfall regime is sub-continental with a dry season during winter, the main maximum precipitation occurs during fall and a secondary maximum during spring-summer (Devoli et al., 2018); convective precipitations are very frequent from late spring to early fall. Pavan et al. (2018) reconstructed rainfall climatology over Po valley from gauges observations ~~since~~ from 1961 to 2015, showing that, although the ~~relative~~ relatively small extent of the ~~study areas here considered~~whole study areas, there are different precipitation regimes between ~~areas~~ the area A1, located close to the Alps, (wetter) and the area A2, the flats south of Torino hill, (dryer). It is worth mentioning that the average annual rainfall within each single study areas is homogeneous.

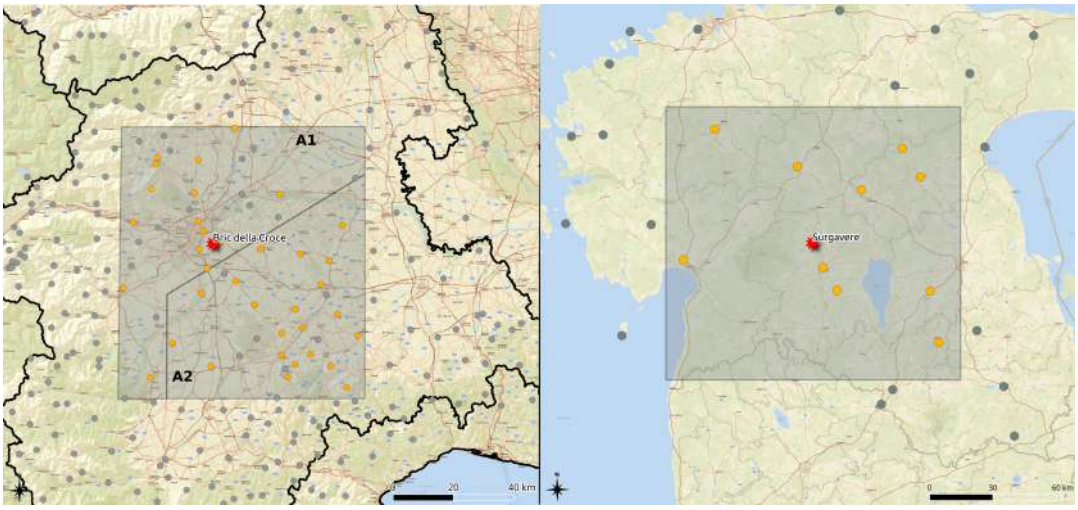

Figure 1. The study areas. On the left the two Italian study areas (EPSG:32632), on the right the Estonian area (EPSG: 3301). The dots symbols show the tipping-bucket raingauges of ~~regional~~ the local hydrological ~~network~~networks, orange dots symbols are the tipping-bucket raingauges used in the study, the red ~~star is~~ stars are the weather radar location, respectively the Bric della Croce radar site and Sűrgavere radar location; basemap: ESRI, https://basemaps.arcgis.com/arcgis/rest/services/World_Basemap_v2/VectorTileServer accessed on 5 November 2022

The Bric della Croce weather radar, operated by the regional agency for ~~the~~ environment protection (Arpa Piemonte) is located on the top of Torino hill. The operational radar completes fully polarimetric volume scans, made of eleven elevations up to 170 km range with 340 m range bin resolution. Quantitative precipitation estimates (QPEs), based on horizontal reflectivity, are extensively described by Cremonini and Tiranti (2018), meanwhile, K_{dp} based precipitation estimations are derived according to Wang and Chandrasekar (2009). The closest observations to the weather radar (up to eight kilometers) ~~has~~ have been left out

due to heavy ground clutter contamination and unreliable estimations of K_{dp}. Being focused on convective precipitation, this study limits the analysis to the warm season ranging in Italy from April to October. Bric della Croce data range from 2014 to 2020 with five minutes interval time resolution. The data inspection for quality purposes has shown that the annual maxima for the years 2015 and 2016 are unreliable, due to frequent weather radar failures during the warm season: for this reason, these years have been excluded from the following analysis.

Arpa Piemonte also operates an automated ground weather network made by more than 350 raingauges with 0.2 mm resolution and 300 mm/h maximum detectable rainfall intensity: one-minute rainfall observations are available since 1988. Annual hourly rainfall maxima are derived from gauges observations corrected for underestimations at high rainfall intensities according to ~~Lanza et al. (2010); Vuerich (2009)~~Lanza et al. (2010) and Vuerich (2009). Annual hourly rainfall maxima are manually quality controlled to identify possible mechanical failures and incomplete time-series. In this work, one-minute resolution tipping-bucket raingauges located within the two study areas and running for at least 15 years have been used. ~~The Area 1 (~~Area A1 ~~)~~ north and west ~~to~~ of the weather radar site contains 27(16) gauges, while ~~the Area 2 (~~area A2 ~~)~~ contains 25(20) gauges; the annual hourly precipitation maxima for all gauges considered in this study range from 1988 to 2020. ~~Annual precipitation maxima derived from raingaugesconfirm different precipitation regimes in~~ After data inspection for anomalous values or outliers to get high quality annual rainfall maxima recorded by raingauges, the present studly is limited to considering 16 gauges for area A1 and 20 ones for area A2. Homogeneity tests have been also applied to evaluate the statistical coherence of the two study areas. Broadly used procedures for testing for regional homogeneity assessment are described and compared in Viglione et al. (2007). In this study, the L-moment homogeneity test (Hosking and Wallis, 1997) has been applied in both areas obtaining H-values less than one, considered as "acceptably homogeneous". The Anderson-Darling (ADAD) rank test (Viglione et al., 2007) also confirms the previous results; they can be explained by the relatively small surface areas considered in this study (about $60 \times 60\, km^2$ for each study area) and by their homogeneity in term of precipitation regimes and geomorphological characteristics.

~~Study~~ The study area in Estonia is centered on the continental part of the country and it extends for about 70 km around the radar corresponding to 16,911 km^2. Estonia is a flat country with a mean elevation of about 50 m a.s.l. and the highest point being 318 m a.s.l in the more hilly southeast (Figure ~~??~~1, right map). Estonia has a temperate climate with the heaviest rainfall in late summer. Convective precipitation is common in the area from May to September ~~(?)~~(Voormansik et al., 2021b) . There are distinct differences in precipitation climate between continental Estonia and the ~~coastal areas and islands~~ islands in the western part as the latter ~~are~~ is much drier (Tammets and Jaagus, 2013). This variance is caused by different thermal regimes of sea and land surfaces. Sub-daily rainfall extremes in the Nordic-Baltic region from rain gauges were analysed by Olsson et al. (2022). They found the 1-hour return level to be uniform in the central part of Estonia without significant variations of the shape parameter, being close to zero. In the study area, we can thus expect a uniform precipitation regime.

~~The Estonian study area (shaded): dots weighted raingauges of regional hydrological network, orange dots weighted raingauges used in the study, pink star Sűrgavere radar location.~~

Sűrgavere radar is situated in the northern part of Sakala upland on top of Sűrgavere hill (128 m a.s.l.). Sűrgavere radar has been operational since 2008 and a continuous archive is available since 2010. Until May 2020, the radar performed a volume scan with eight elevations up to 250 km range with 300 m range bin resolution every 15 minutes. In May 2020 the scan strategy received a major update. Since then the radar scans seven elevations with a 250 km range every five minutes and the lowest elevation with a 250 km range every 2.5 minutes. After careful inspection of reflectivity and polarimetric data quality~~5~~, five years of radar data (2012-2013 and 2018-2020) were included in the study. ~~Mean radar data availability for the investigated period were 98%.~~ Data from 2014, 2015, and 2017 ~~was~~ were not included because of insufficient polarimetric data quality to obtain reliable QPEs. ~~the~~ 2014 and 2015 were excluded because of a broken waveguide limiter which caused gradually decreasing polarimetric data quality. Data from 2017 was left out because a broken stable local oscillator (STALO) reduced the data quality to levels not usable for QPE purposes. The year 2016 was omitted because of the low availability of radar data due to frequent and long-lasting radar failures (availability of 30% for August and 85% for the whole summer period of that year) ~~. Only 15 minute~~ that would result in unreliable annual maxima. Mean radar data availability for the investigated five year period was 98%. Only 15-minutes interval data is used in this study to maintain homogeneity.

K_{dp} precipitation estimates of Estonia are derived using PyART function *phase_proc_lp* (Giangrande et al., 2013). Compared to the work by ~~? done on~~ Voormansik et al. (2021a) done in the same study area some parameters of this function have been changed. The necessity of updating the parameters became inevitable because using the parameters of the earlier work ~~leaded~~ led to unrealistically high ~~1 hour~~ 1-hour rainfall maxima and ~~oversmoothed~~ over smoothed precipitation fields. The parameters of the function that were changed were *window_len*, *high_z*, and *coeff*. The first of these, *window_len*, allows ~~to change~~ changing the length of the Sobel window applied to Φ_{dp} field ~~when prior to~~ before calculating K_{dp}. When using the default window length of 35, the function produces less accurate results in K_{dp} fields with steep gradients and large K_{dp} magnitudes as it oversmooths the Φ_{dp} field (Reimel and Kumjian, 2021). We tested with various window lengths and found length 8 to be the optimal compromise between spatial resolution and smoothness. After the window length change, we obtained realistic-looking precipitation fields but the overestimation compared to gauge values increased. This is because Φ_{dp} gradients became ~~more steep~~ steeper as a result of the smaller window length. To mitigate this issue we first decreased the *high_z* (high limit for reflectivity to remove hail contamination) value from 60 dBZ used in ~~?~~ Voormansik et al. (2021a) to 50 dBZ which is the lowest recommended value by Giangrande et al. (2013). Because overestimation was still evident we also reduced the Z_h-K_{dp} ~~self consistency~~ self-consistency coefficient. As stated by Kumjian et al. (2019) the Z_h-K_{dp} consistency relationships probably do not exist in hail and it is therefore recommended to reduce the weight of the self-consistency constraint in the case of hail ~~Reimel and Kumjian (2021)~~(Reimel and Kumjian, 2021). We tested with various values and found the coefficient value of 0.9 to produce the optimal results.

The following equations have been used to derive rain rate from weather radar variables:

$$R(Z_h) = 300Z^{1.5} \quad (1)$$

and

$$R(K_{dp}) = 21.0 K_{dp}^{0.720} \tag{2}$$

Horizontal reflectivity data is re-calibrated using a method that makes use of the knowledge that Z_h, Z_{dr} (differential reflectivity), and K_{dp} are self-consistent with one another and one can be computed from two of the others. The calibration was carried out using the theory set down in Gorgucci et al. (1992) and Gourley et al. (2009) where the process is described in detail. As a result, Z_h bias of 2.0 to 5.0 dB depending on the data period is obtained and added to the corresponding original reflectivity data. Data up to 10 km from the radar were excluded because of the ground clutter and unreliable K_{dp} estimation. Weighted rain gauges operated by the Estonian Environment Agency (EstEA) located in the study area are used as ground truth to compare with radar estimates. The rain gauges provide data with a resolution of 0.1 mm and maximum detectable rainfall intensity of 2000 mm/h. Rainfall observations from 2003-2010 are available with ~~1 hour~~ 1-hour resolution and starting from 2011 with ~~10 minute~~ 10-minutes interval. The data are manually quality controlled by EstEA staff to identify possible technical issues or incomplete ~~time-series~~time series. In this study ~~10~~ ten years of gauge data from 10 stations located in the study area from ~~2011-2020~~ 2011 to 2020 are used. As demonstrated by **?**Voormansik et al. (2021a), the combined product $R(Z_h, K_{dp})$ outperforms with respect to QPEs based on $R(Z_h)$ and $R(K_{dp})$. The weather ~~radar based~~ radar-based QPE here used is defined as:

$$R(Z_h, K_{dp}) = \begin{cases} R(Z_h), & \text{if } Z_h \leq 25 \quad \text{dBZ} \\ R(K_{dp}), & \text{otherwise} \end{cases} \tag{3}$$

The evaluation of horizontal reflectivity threshold has been derived optimizing results on 1-hour accumulation rainfall in both locations, Italy and Estonia (Voormansik et al., 2021b).

2.1.1 GEV Statistics

Extreme value theory (EVT) deals with the stochasticity of natural variability by describing extreme events ~~with respect to~~ concerning a probability of occurrence. The frequency of occurrence for events with varying magnitudes can be described as a series of identically distributed random variables

$$F = X_1, X_2, X_3, ...X_N \tag{4}$$

where F is some function that approximates the relationship between the magnitude of the event (variable X_N) and the probability of its occurrence. EVT is one of the most recurrent ~~methodology~~ methodologies used for the statistical description of rare events. Extensive literature, dating back to the 1940s, deals with EVT in its formalization and its hydrological applications. Looking at the distribution of block maxima (a block is defined as a set ~~time~~ period such as a year), the Generalized Extreme Value (GEV) distribution is one of the most popular ~~its~~ fundamental approaches: the introduction theory and ~~an~~ a historical

review on this topic can be found in Papalexiou et al. (2013), Wilks (2011), de Haan and Ferreira (2006). According to Katz et al. (2002), the GEV distribution, which combines three different statistical families (Gumbel, Fréchet, and Weibull), can fit the extreme data set with ~~a~~ high accuracy.

Defining R_{1h} as the random variable of annual maximum rainfall intensity for the hourly duration, it is expected that random samples of annual maxima are distributed as the GEV cumulative distribution function $F(x)$ (Jenkinson, 1955):

$$F(R_{1h} \leq x; \mu, \sigma, \xi) = \begin{cases} e^{-[1+\xi\frac{x-\mu}{\sigma}]^{\frac{-1}{\xi}}} & \xi \neq 0 \\ e^{-e^{\frac{-(x-\mu}{\sigma}}} & \xi = 0 \end{cases} \quad (5)$$

where three parameters, μ, σ and ξ represent respectively ~~a~~ the location, scale, and shape of the distribution function. Note that σ and $1+\xi(x-\mu)/\sigma$ must be greater than zero, while the shape and location parameters can take on any real value. The shape parameter ξ governs the three limiting distributions of extreme values:

- $\xi > 0$ Fréchet distribution (EV2);
- $\xi = 0$ Gumbel distribution (EV1);
- $\xi < 0$ Weibull distribution (EV3).

The GEV distribution unites the Gumbel, Fréchet, and Weibull distributions into a single family to allow a continuous range of possible shapes (Frűh et al., 2010; Coles, 2001). These three distributions are known as type I, II, and III extreme value distributions. The GEV distribution is parameterized with a location parameter (μ), scale parameter ($\sigma > 0$), and shape parameter (ξ). The GEV is equivalent to type I, II, and III, respectively, when a shape parameter is equal to zero, greater than zero, and lower than zero. Based on the extreme value theorem, the GEV distribution is the limit distribution of properly normalized maxima of a sequence of independent and identically distributed random variables. Thus, the GEV distribution is used as an approximation to model the maxima of long (finite) sequences of random variables.

Several methods have been developed for the estimation of GEV distribution parameters, including the method of moments (MME), the method of L-moments (LME), the method of ~~probability weighted~~ probability-weighted moments (PWME), and the method of maximum likelihood (MLE) (Katz et al., 2002; de Haan and Ferreira , 2006). Hereafter, the only MLE method has been used to estimate GEV distribution parameters from sample data.

Quantiles associated with the T-year return period $T = 1/1\text{-}F(r_{1h} \leq x)$ are determined by inverting the GEV cumulative distribution function given by Eq. (5).

The shape parameter controls the upper-tail behavior, but it remains difficult to estimate on the basis of short time-series data (few decades for example): it happens because there are usually few extremes exhibiting much variability. As stated by Lazoglou et al. (2018), the Weibull (negative shape parameter) is not appropriate for precipitation ~~dataset~~datasets. Moreover, Ragulina and Reitan (2017) demonstrated that small countries or administrative regions within larger countries can be assigned roughly the same shape parameter, but larger areas such as continents can be expected to be heterogeneous. As a result of their

work, ~~that~~ which considered 1,495 stations worldwide, the global average for the shape parameter is equal to 0.139, with a 99% credibility interval ranging from 0.127 to 0.150. The weather radar-based rainfall annual maxima statistics over the Netherlands calculated by Overeem et al. (2009a) have ~~been~~ shown that regional differences in the GEV location parameter exist for ~~most duration~~the most durations. Nevertheless, due to the small number of rainfall annual maxima, when depth-duration-frequency (DDF) curves are derived for small areas, the uncertainties in the DDF curves generally become larger compared to the uncertainties of the average DDF curve for the Netherlands. ~~Moreover, as~~ Recalling an increase in the standard errors of the quantile estimates, in particular at high return periods, Bruishand (1991) underlies that large standard errors are mainly caused by the uncertainty in the shape parameter. Assuming that the shape parameter does not vary across the study areas, Bruishand (1991) shows that a better estimate of large quantiles can be obtained by and estimating the common shape parameter by averaging the at-site estimates. On the other side, real-time operational applications, like early warnings, are based on relatively low quantiles (typically 10-20 years return period). Within for these range of return periods the inaccuracy is expected to be considerably reduced (Marra et. al., 2019). For these reason in this study, Gumbel distribution ($\xi = 0$) have been assumed appropriate for annual rainfall maxima.

As discussed by Overeem et al. (2009a), the spatial correlation of measurements affects extreme values statistics, carrying to underestimation. The correlation between two raingauges is typically low for convective precipitation, due to the small spatial scales involved in convection ($\approx 10 - 100\,km^2$) and the low density of the ground meteorological network (typically order of one gauge every $100\,km^2$). In the case of weather radar observations, given the higher spatial resolution ($\approx 1\,km^2$), the correlation between close ~~cells~~ cell grids must be estimated and taken into account. ~~In this study the statistical analysis has been conducted using the R () package ExtRemes 2.1 (Gilleland et al., 2016).~~

3 ~~Results~~

~~Assuming GEV~~ Assuming GEV distribution parameters are constant in each ~~areas~~ of area considered in this study, their estimation from all data in the regions justifies the derivation of return periods longer than the rainfall record (Overeem et al., 2010). This statement assumes that both sample data are independent and the precipitation regime in the studied area is uniform. To avoid data spatial correlations, this studly merely investigates 1-hour rainfall totals, diseregarding longer durations.

Semi-variograms are widely used in geostatistic sciences for evaluating rainfall spatial structure. Semi-variograms summarize the spatial relations in the data, and they can be used to understand within what range data are spatially ~~autocorrelated (Naimi et al., 2011).~~correlated (Naimi et al., 2011).

In this study, the statistical analysis has been conducted using the R (https://cran.r-project.org/) package ExtRemes 2.1 (Gilleland et al., 2016). The experimental isotropic semi-variogram can be derived by taking half the average of the squared difference between data pairs at equal ~~distance~~ distances and by assuming stationarity and isotropy of the rainfall field (Cressie, 1993):

$$\gamma(h) = \frac{1}{2n(|h|)} \sum_{k=1}^{n(|h|)} (z(x_k + h) - z(x_k))^2 \quad (6)$$

where x_k is the location of cell barycentre k and $x_k + h$ ~~the locations~~ is the location at distance h from location x_k. ~~The Figure ??~~ Figure 2 shows semi-variograms, obtained from ~~$Z - K_{dp}$~~ $R(Z_h, K_{dp})$ annual hourly rainfall maxima, from April to September in Italy for Area 1 (left) and Estonia (right).

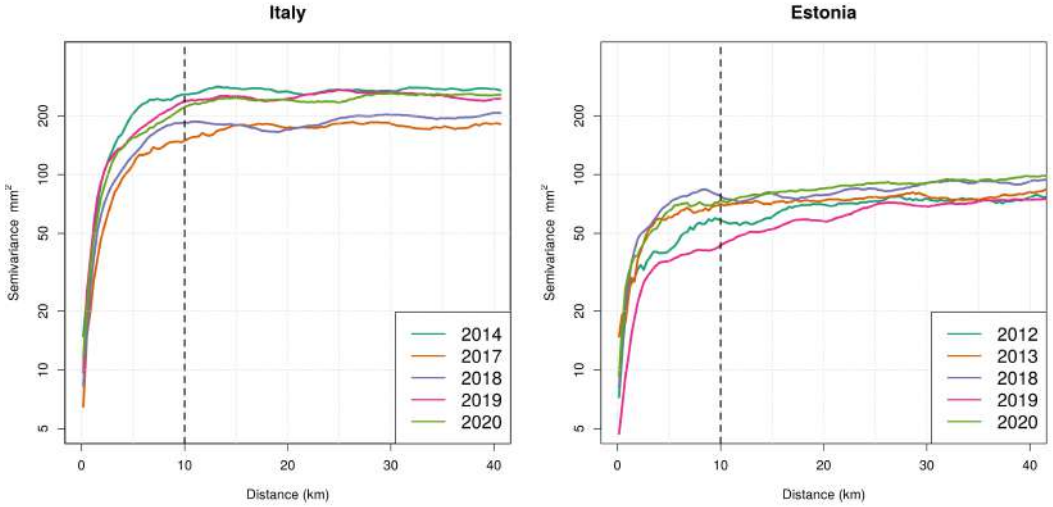

Figure 2. Empirical variograms for hourly rainfall annual maxima based on ~~$Z - K_{dp}$~~ $R(Z_h, K_{dp})$ hourly rainfall estimations in Italy Area 1 (left) and Estonia (right).

The empirical semi-variogram analysis for weather radar observations indicates that hourly rainfall maxima decorrelate at about 10 km both in Estonia and Italy (Figure **??**~~): this result confirms that during the warm season~~ 2). These results are consistent with past studies (Schroeer et al., 2018; Dzotsi et al., 2012): convective precipitation is prevalent during the warm season and, consequently, the spatial correlation quickly decreases with the distance between two ~~points. Ten~~ rain gauges. Moreover, ten kilometers is the typical spatial scale of convective precipitation systems ($meso - \gamma$). Different values of semi-variances in Estonia and Italy can be explained by the different climatic regimes, with generally weaker convective precipitations in the Baltic country. Hence, to avoid statistical oversampling and to ensure statistical ~~independent data sample, annual hourly maxima precipitations~~ independence of data samples, 1-hour rainfall total annual maxima estimated by weather radar are re-sampled according to the found spatial scale of convective precipitation. The hourly annual rainfall maxima estimated by weather radar observations are up-scaled from the original data resolution (340 meters for Italy and 300 meters for Estonia) to 10 km resolution, using a uniform random sampling algorithm. ~~The GEV distribution unites the Gumbel, Fréchet and Weibull distributions into a single family to allow a continuous range of possible shapes. These three distributions are~~

known as type I, II and III extreme value distributions. The GEV distribution is parameterized with a location parameter (μ), scale parameter ($\sigma > 0$) and shape parameter (ξ). The GEV is equivalent to the type I, II and III, respectively, when a shape parameter is equal to zero, greater than zero, and lower than zero. Based on the extreme value theorem, the GEV distribution is the limit distribution of properly normalized maxima of a sequence of independent and identically distributed random variables. Thus, the GEV distribution is used as an approximation to model the maxima of long (finite) sequences of random variables.

Diagnostic plots for 1-hour annual rainfall maxima fits derived by weather radar in Italy Area 1 (upper) and Estonia (lower): density plot, P-P plot, Q-Q plot

3 Results

The Figure 3 shows the diagnostics from the GEV df Gumbel distribution fitted to 1-hour annual maxima rainfall in Italy Area 1 rainfall total annual maxima in Italy for area A1 (upper) and Estonia (lower), derived from $R(Z_h, K_{dp})$ estimates; from left to right, the Figure shows the density plot of empirical data and fitted GEV df, quantiles from a sample drawn from the fitted GEV df against the empirical data quantiles the data along with the model fitted density, the Q-Q plot of the data quantiles against the fitted model quantiles with 95% confidence bandsand Quantile-Quantile (, a Q-Q) plot (top left) are reportedplot of quantiles from model-simulated data against the data. Quantile-quantile (Q–Q) scatterplots compare empirical data and fitted CDFs in terms of quantiles: in an ideal perfect fitting, all points should lay on the 1:1 diagonal line (Wilks, 2011).

The Q-Q plots present some departures from linearity in correspondence of the tails, especially for Estonia data, which are due to the increasing level of uncertainty that characterizes model extrapolation at high levels. The empirical estimates in the return level plot reflect results in Q-Q plots laying very close to the model based model-based line, which results to be almost linear, for low values. However, even if the return level estimates seem convincing, the increasing confidence bands for large return periods indicate the uncertainty that affects the model at high levels.

The Table 1 summarizes the results of fitting data samples with GEV distribution applying Gumbel distribution by applying the Maximum Likelihood Estimation method (MLE) for each studied area. Values for location , scale and shape ; location and scale parameters with their standard deviations errors ($\sigma/sqrt(n)$) are shown. Most of shape parameters are close to zero, indicating a theoretical Gumbel distribution as expected. Significant exceptions are the negative value for study area 1 in Italy for GEV fit derived by raingauges, and the positive value for Estonia fit derived from the weather radarKolmogorov-Smirnov tests (Ks-test) and Q-Q plots inspections (Wilks, 2011) show that fits for $R(Z_h, K_{dp}$ a more reliable than $R(Z_h)$ ones in all the three study areas. This behaviour is particularly evident for Estonia area, where the fit distribution for $R(Z_h)$ leads to large value of the scale parameter and anomalous low p-value obtained by KS-test.

The record length strongly It is well-known that record length affects the estimate of the GEV shape parameter and long historical time series are needed for reliable estimates. Papalexiou et al. (2013), Ragulina and Reitan (2017), Lazoglou et al. (2018), Lutz et al. (2020), Deidda et al. (2021) demonstrated that the shape parameter tends to have positive values, between 0 and 0.23 with probability a probability of 99%, as sample size increases. For Estonia, the shape parameter ξ positive ($+0.12 \pm 0.02$) derived from weather radar is in agreement with findings in extreme value rainfall analysis of these studies

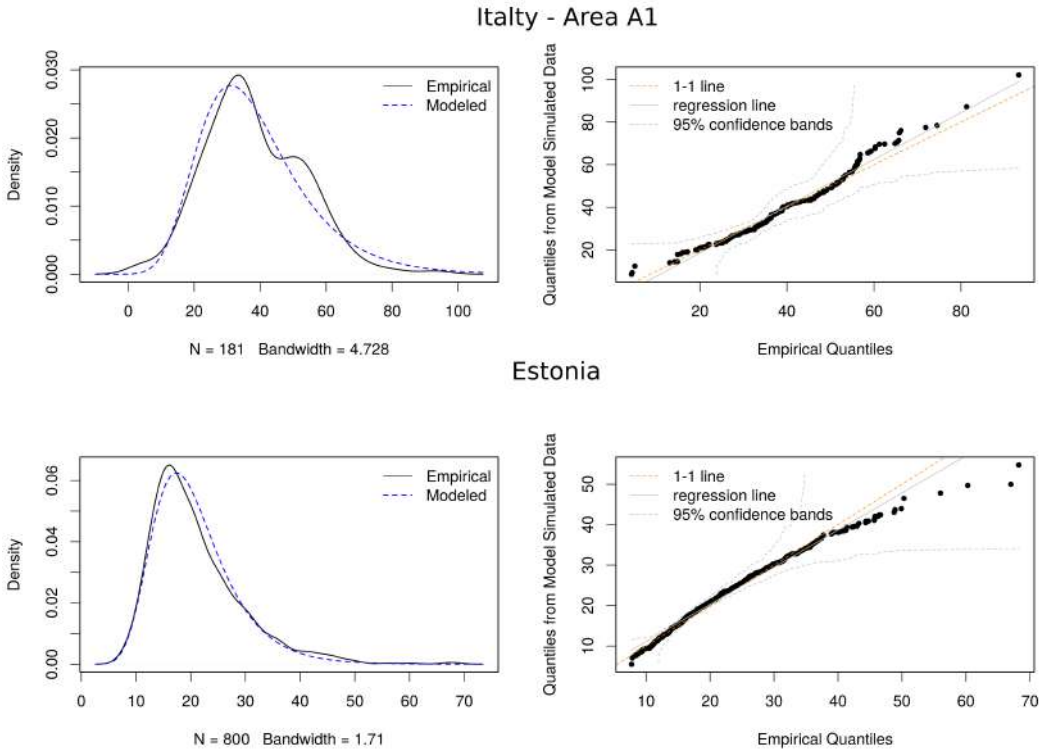

Figure 3. Diagnostic plots for 1-hour annual rainfall maxima fits derived by weather radar in Italy Area 1 (upper) and Estonia (lower): from left to right, density plot of the data along with the model fitted density, Q-Q plot of the data quantiles against the fitted model quantiles with 95% confidence bands, a Q-Q plot of quantiles from model-simulated data against the data.

~~(Ragulina and Reitan, 2017). On the other side, close to zero values for shape parameters estimated by Italian weather radar observations can be explained by the limited sample size~~However, in this study, given the shortness of the weather radar time series, for safety the scale parameter has been set to zero, according to Papalexiou et al. (2013).

4 Discussion

Several studies developed adjustment techniques to correct QPEs based on weather radar observations with rain gauges measurements (Einfalt and Michaelides , 2008; Goudenhoofdt and Delobbe, 2009). For the first time, this study investigates extreme precipitation estimation using ~~dual-pol~~ dual-polarization weather radar rainfall estimations without any adjustment with raingauges. It is worth recalling that the study has been limited to relatively flat ~~areas with high quality~~ and geomorphologically homogeneous areas with high-quality dual-polarization weather radar observations close to the ground ~~. Data~~ and high quality 1-hour rainfall total annual maxima from raingauges. Weather radar data quality and reliability have been carefully checked in Voormansik et al. (2021a).

Area	Source	μ (mm)	σ	~~ξ~~ n-values
Italy - A1	WR-KDP	31.4 ± 1.0	13.3 ± 0.7	181
	~~226~~ WR-ZH	19.2 ± 0.7	9.5 ± 0.6	181
	RG	31.2 ± 0.8	12.7 ± 0.6	~~609~~ 297
Italy - A2	WR-KDP	30.4 ± 0.9	11.0 ± 0.7	164
	~~235~~ WR-ZH	18.0 ± 0.6	7.7 ± 0.5	164
	RG	25.0 ± 0.5	9.9 ± 0.4	~~595~~ 484
Estonia	WR-KDP	17.4 ± 0.2	5.9 ± 0.1	800
	~~809~~ WR-ZH	14.6 ± 0.3	6.8 ± 0.2	800
	RG	15.1 ± 0.6	5.9 ± 0.5	93

Table 1. Estimated ~~GEV~~ Gumbel parameters, location ~~, scale~~ and ~~shape~~ scale (μ,~~σ,ξ~~μ,σ) for weather radar and gauges annual hourly maxima rainfall intensities for Italy Area 1 and Area 2 and Estonia for weather radar derived from $R(Z_h, K_{dp})$ (~~WR~~WR-KDP), derived from $R(Z_h)$ (WR-ZH) and raingauges (RG) ~~time series~~ time-series observations

The two studied regions, Estonia and Italy, are ~~characterised~~ characterized by different precipitation regimes, colder the first one ~~,~~ and warmer the latter. ~~Different~~ The different climate regimes of ~~studies~~ the studied areas consequently reflect on ~~GEV estimations~~fitted Gumbel distributions, determining lower return periods in Italy, given ~~hourly precipitations~~1-hour rainfall total. Estonia is ~~characterised by few rainguages~~ characterized by few rain gauges and by a limited historical series, but also by a larger homogeneous flat region covered by the operational polarimetric weather radar. In this area, it can be appreciated the benefit of estimating ~~GEV~~ Gumbel distribution using weather radar observations after ensuring the spatial independence and assumed homogeneity: the sample size derived from five years observations is ~~made by 809 values,~~ about nine times the sample size obtained by raingauges. These different sample sizes determine larger standard deviations in ~~GEV~~ Gumbel distribution parameters estimation by raingauges with respect to weather ~~radar~~radar-based estimations.

In Italy, ~~an opposite condition is evident:~~ a dense automatic gauges network is operating since 1988, providing about ~~30~~ 20 gauges per area~~and more than 600 values~~ , determining larger sample size. But, ~~The~~ the Alps and the spatial variability of the climate regime, influenced by complex orography, ~~limits the available weather radar based sample to about 250~~ limit the availability of high-quality weather radar observations to about 160-180 values. Despite the limited availability of weather radar observations (only five years for both Italian and Estonian weather radars), the comparison of ~~GEV~~ Gumbel distribution fits in these two different regions has shown encouraging results.

~~The~~ Figure 4 shows return levels for ~~one~~ 1hour rainfall at a given return time, estimated from ~~GEV~~ Gumbel distributions with location ~~, shape and scale~~ and shape parameters from Table 1 ~~. In Italy~~ for the study areas and estimated from $R(Z_h)$, $R(Z_h, K_{dp})$ and from raingauegs.

In Italy, the different return periods between the two areas are in agreement with findings in Mezzoglio et al. (2022) and with climate classification of the two areas reported by Pavan et al. (2018), with Area 1 more ~~favourable~~ favorable to intense

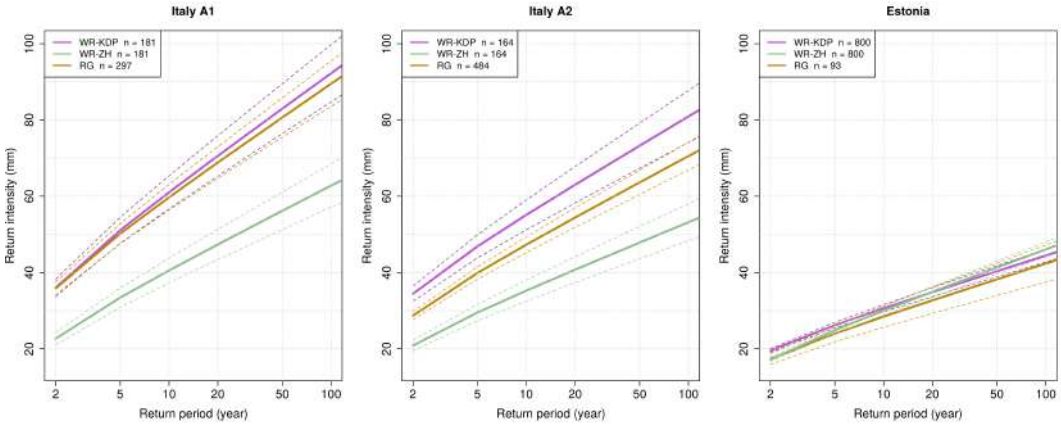

Figure 4. Return levels for 1-hour rainfall accumulation in Estonia (left) and Italy Area 1 (center) and Area 2 (right) derived from the Gumbel distributions.The dash lines show confidence intervals for $\alpha = 0.05$.

precipitation than Area 2. This ~~condition~~precipitation regime, confirmed also by climatological lightning density (not shown), ~~is caused by local orography~~can be justified by local geomorphology. In fact, during the warm season, cold air overcomes the Alps flowing towards the Po valley from west-northwest: the Monferrato hills east of Torino ~~enhances low~~enhance low-level convergences and strong uplifts, causing deep convection in ~~the Area 1.~~ area A1, while the area A2 experiences downwind conditions. QPEs based on $Z_h - K_{dp}$ ~~generally provided~~ algorithm generally provided slight shorter return periods with respect to gauges estimations, probably due to a slight overestimation of annual rainfall maxima by weather radars, as highlighted by ~~?~~Voormansik et al. (2021a). Distribution fits based on $R(Z_h)$ show longer return period, given 1-hour rainfall total, in all three areas. This return period overestimation is dramatic in Italy where higher 1-hour rainfall maxima total are expected. The following Table summarizes the return time periods estimates for 1-hour rainfall accumulation for the three study areas, derived from $R(Z_h)$, $R(Z_h, K_{dp})$ and from raingauegs.

Return period	Italy A1			Italy A2			Estonia		0.5ex>0.5ex
	WR-KDP	WR-ZH	RG	WR-KDP	WR-ZH	RG	WR-KDP	WR-ZH	RG0.5ex>0.5ex
2	36	23	36	34	20	29	20	17	17
10	61	41	60	55	35	47	31	30	29
20	71	47	69	63	40	54	30	35	33
50	83	56	81	73	48	64	40	41	38
100	92	63	90	81	53	71	44	46	421ex>1ex

Table 2. The return time periods estimates for 1-hour rainfall accumulation for the three study areas, derived from $R(Z_h)$, $R(Z_h, K_{dp})$ and from raingauegs

The maxima 1-hour accumulation for given return time obtained from $R(Z_h, K_{dp})$ show better agreement with values obtained by raingauges. In the two Italian areas, the underestimation by $R(Z_h)$ is evident and larger in area A1 than in area A2. For Estonia, $R(Z_h, K_{dp})$ confirms good performance, while $R(Z_h)$ confirms underestimation but it also shows an unrealistic large scale parameter and a low statistical significance of the fit. Recalling the findings in Voormansik et al. (2021a), QPEs derived by Z_h show underestimation during the warm season. However, several reasons can explain the weakness of $R(Z_h)$:

1. horizontal radar reflectivity attenuation cause by intense instantaneous rainfall rates;
2. partial beam-filling;
3. inappropriate reflectivity cap threshold (55 dBZ) to avoid hail contamination. Disdrometer measurements reported cases of rainfall rates greater than 100 mm/h;
4. clutter residual;
5. inappropriate drop size distribution assumed to convert weather radar horizontal reflectivity in rain rate.

On the other side, $R(Z_h, K_{dp})$ estimations outperform in strongly convective precipitations regime like in Northern Italy, being immune from hail contamination and rainfall attenuation.

5 Conclusions

Several studies investigated rainfall annual maxima derived from weather radarbased QPEs obtained by the traditional $Z_h - R$ relationship with some adjustments with raingauges. ~~Nevertheless, as stated by Barndes et al. (2001) and ?~~Since the past decades, dual polarization weather data radar observations are becoming available from operational weather radars. As stated by Bringi and Chandrasekhar (2001) and Voormansik et al. (2021a), the benefits of using dual polarization variables like K_{dp} in rainfall estimates are evident: these QPEs are immune from weather radar miscalibration, anomalous propagation~~and partial beam blockings~~, and partial beam-blockings or beam-filling.

For the first time, this study investigates QPEs based on polarimetric observations by operational C-band weather radar located in Italy and ~~in~~ Estonia. As shown by ~~?~~Voormansik et al. (2021a), rainfall estimations based on $Z_h - K_{dp}$ algorithms are robust and reliable, overcoming most of ~~sources~~ the sources' uncertainties: hence, no corrections ~~neither~~ nor adjustments with raingauges have been applied. The annual maximum of 1-hour rainfall accumulation is typically assumed to have general extreme value (GEV) distribution. Given the shortness of weather radar data, this study is limited to a short duration (1-hour) in homogeneous regions assuming parent Gumbel distributions. Hence, Gumbel distribution parameters and depth-frequency curves have been derived from the 1-hour dual-pol weather radar-based annual rainfall maxima. The comparison of weather radar return period estimations with ones derived from ~~longterm~~ gauges observations showed a good agreement. ~~From 1-hour annual rainfall maxima GEV distributions parameters and depth-duration-frequency curves have been derived. Moreover, this~~ This study demonstrates that ~~,~~thanks to weather radar's high spatial resolution, even ~~limited~~ a limitedtime series of weather

radar observations can provide reliable estimations of ~~GEV parameters~~ extreme values distribution parameters for annual hourly rainfall maxima in climatological homogeneous regions. It is worth ~~to recall~~ recalling that QPEs based on ~~$Z_h - K_{dp}$~~ $R(Z_h - K_{dp})$ observations can be obtained only in cases of warmseason precipitations (anyway, when most intense precipitations occur). The shown results demonstrate good agreement between ~~weather radar~~ QPEs obtained by $R(Z_h - K_{dp})$ and raingauges data and consistent estimations of ~~GEV~~ Gumbel distribution parameters. ~~Moreover, this study shows~~ Assuming homogeneous regions with high quality weather radar observations, it is shown that even limited time-series weather radar observations ~~are able to discriminate~~ can discriminate 1-hour rainfall total annual maxima between different precipitation regimes. ~~This~~ These results are promising especially if we recall that the two areas in Italy are ~~characterised~~ characterized by slightly different precipitation regimes and the applied statistical analysis ~~is able to describe~~ can describe them properly. The main requirements for weather radar observations applying this approach consist ~~in~~ of a proper weather radar calibration, radar visibility~~and~~ , and a limited beam-broadening united to ~~weather observations close to~~ limited beam height above the ground. Sub-hourly precipitation extremes can determine a wide range of impacts on infrastructure, economy, and even health causing urban flooding, ~~trigger~~ triggering landslides, flash floods, and heavy soil erosion. Hence, future works will ~~be~~ investigate sub-hourly rainfall accumulation intervals, estimating GEV ~~parameters~~ parameter distributions and deriving other significant return periods. More dual-polarized meteorological data will become available in the coming years, allowing investigations of longer durations and shape parameters over larger areas.

Code and data availability. The code used to conduct all analyses, raingauges and weather radar data used in this study are available by contacting the authors.

Author contributions. R.C., T.V., D.M. and P.P. contributed to the design and implementation of the research, to the analysis of the results and to the writing of the manuscript. All authors read and approved the manuscript.

Competing interests. The authors declare no conflict of interest.

Acknowledgements. This research has been supported by the Estonian Research Council (grant no. PSG202). All figures included in the study were produced by the use of Free and Open Source Software (i.e. Quantum GIS Geographic Information System - Open Source Geospatial Foundation Project, http://qgis.osgeo.org, and the R Project for Statistical Computing, https://www.R-project.org/).

References

Allen, R. J., and A. T. De Gaetano (2005b), Considerations for the use of radar-derived precipitation estimates in determining return intervals for extreme areal precipitation amounts, J. Hydrol., 315, 203–219, doi:10.1016/j.jhydrol.2005.03.028.

T. A. Bruishand (1991) Extreme rainfall estimation by combining data from several sites, Hydrological Sciences Journal, 36:4, 345-365, DOI: 10.1080/02626669109492519

Coles, S (2001): An Introduction to Statistical Modeling of Extreme Values. Springer Series in Statistics. Springer Verlag London. 208p

Delrieu, G., Andrieu, H. and Creutin, J.D. (2000). Quantification of path-integrated attenuation for X-and C-band weather radar systems operating in Mediterranean heavy rainfall. Journal of Applied Meteorology, 39(6), pp.840-850.

Brandes, E. A., A. V. Ryzhkov, and D. S. Zrnic, 2001: An evaluation of radar rainfall estimates from specific differential phase.J. Atmos. Oceanic Technol.,18, 363–375, doi:10.1175/1520-0426(2001)018,0363:AEORRE.2.0.CO;2

Bringi, V. N. and Chandrasekhar, V.: Polarimetric Doppler Weather Radar. Principles and Applications. Cambridge University Press, NY, 636 pp., 2001.

Cressie, N. A.: Statistics for spatial data, Wiley, NY, revised edn., 1993. 2090

Cremonini, R. and Bechini, R. Heavy rainfall monitoring by polarimetric C-Band weather radars. Water 2010, 2, 838-848.

Cremonini, R. and Tiranti, D. (2018) The Weather Radar Observations Applied to Shallow Landslides Prediction: A Case Study From North-Western Italy, Frontiers in Earth Science, 6, 134, https://www.frontiersin.org/article/10.3389/feart.2018.00134, doi:10.3389/feart.2018.00134,ISSN:2296-6463

Deidda, R., Hellies, M. and Langousis, A. A critical analysis of the shortcomings in spatial frequency analysis of rainfall extremes based on homogeneous regions and a comparison with a hierarchical boundaryless approach. Stoch Environ Res Risk Assess (2021). https://doi.org/10.1007/s00477-021-02008-x

Devoli, G., Tiranti, D., Cremonini, R., Sund, M., and Boje, S.: Comparison of landslide forecasting services in Piedmont (Italy) and Norway, illustrated by events in late spring 2013, Nat. Hazards Earth Syst. Sci., 18, 1351-1372, https://doi.org/10.5194/nhess-18-1351-2018, 2018.

Dzotsi, K. A., Matyas, C. J., Jones, J. W., Baigorria, G., and Hoogenboom, G. (2014). Understanding high resolution space-time variability of rainfall in southwest georgia, United States. International Journal of Climatology, 34(11), 3188–3203. https://doi.org/10.1002/joc.3904

E.J.M. van den Besselaar, A.M.G. Klein Tank, T.A. Buishand Trends in European precipitation extremes over 1951-2010 Int. J. Climatol. 2689 (2012), 10.1002/joc.3619

Einfalt, Thomas and Michaelides, Silas. (2008). Precipitation: Advances in Measurement, Estimation and Prediction. 10.1007/978-3-540-77655-0_5.

Fabry, F., V. Meunier, B.P. Treserras, A. Cournoyer, and B. Nelson, 2017: On the Climatological Use of Radar Data Mosaics: Possibilities and Challenges. Bull. Amer. Meteor. Soc., 98, 2135–2148, https://doi.org/10.1175/BAMS-D-15-00256.1

Fairman, J. G., Jr., D. M. Schultz, D. J. Kirshbaum, S. L. Gray, and A. I. Barrett, 2015: A radar-based rainfall climatology of Great Britain and Ireland. Weather, 70, 153–158, doi:https://doi.org/10.1002/wea.2486

Frederick, R. H., V. A. Myers, and E. P. Auciello (1977), Storm depth-area relations from digitized radar returns, Water Resour. Res., 13, 675–679, doi:10.1029/WR013i003p00675.

Frűh, B., H. Feldmann, H.-J. Panitz, and G. Schädler, D. Jacob, P. Lorenz, and K. Keuler, 2010: Determination of precipitation return values in complex terrain and their evaluation. J. Climate, 23, 2257-2274.

Gilleland E, Katz RW (2016). ExtRemes 2.0: An Extreme Value Analysis Package in R, Journal of Statistical Software, 72(8), 1–39. doi: 10.18637/jss.v072.i08.

Giangrande, S.E., McGraw, R. and Lei, L. (2013). An application of linear programming to polarimetric radar differential phase processing. Journal of Atmospheric and Ocean Technology, 30(8), pp.1716-1729.

Gorgucci, E., Scarchilli, G., and Chandrasekar, V. (1992). Calibration of radars using polarimetric techniques. IEEE transactions on geoscience and remote sensing, 30(5), 853-858.

Goudenhoofdt, E. and Delobbe, L.: Evaluation of radar-gauge merging methods for quantitative precipitation estimates, Hydrol. Earth Syst. Sci., 13, 195–203, doi:10.5194/hess-13-195- 2009, 2009.

Gourley, J. J., Illingworth, A. J., and Tabary, P. (2009). Absolute calibration of radar reflectivity using redundancy of the polarization observations and implied constraints on drop shapes. Journal of Atmospheric and Oceanic Technology, 26(4), 689-703.

de Haan, L. and Ferreira, A. (2006) Extreme Value Theory: An Introduction. Springer, New York. http://dx.doi.org/10.1007/0-387-34471-3

Hosking, J., and J. Wallis (1997), Regional Frequency Analysis: An Approach Based on L-Moments, Cambridge Univ. Press, New York.

Katz, R.W.; Parlange, M.B.; Naveau, P. Statistics of extremes in hydrology. Adv. Water Resour. 2002, 25, 1287–1304.

Keupp, L.; Winterrath, T.; Hollmann, R. Use of Weather Radar Data for Climate Data Records in WMO Regions IV and VI; Technical Report, WMO CCl TT-URSDCM; WMO: Geneva, Switzerland, 2017.

Kumjian, M.R., Lebo, Z.J. and Ward, A.M., 2019. Storms producing large accumulations of small hail. Journal of Applied Meteorology and Climatology, 58(2), pp.341-364. ~~IPCC , 2014~~

IPCC 2021 Summary for Policymakers. In: Climate Change ~~2014: Synthesis Report~~2021: The Physical Science Basis. Contribution of Working ~~Groups I , II and III to the Fifth~~ Group I to the Sixth Assessment Report of the Intergovernmental Panel on Climate Change ~~Core Writing Team, R.K. Pachauri and L.A.Meyer (eds. .IPCC, Geneva, Switzerland, 151 pp~~(MassonDelmotte V., Zhai P., Pirani A., Connors S. L., Péan C., Berger S., Caud N., Chen Y., Goldfarb L., Gomis M. I., Huang M., Leitzell K., Lonnoy E., Matthews J. B. R., Maycock T. K., Waterfield T., Yeleki O., Yu R. & Zhou B., eds.). Cambridge University Press, Cambridge, UK.

Jenkinson, A. F. (1955), The frequency distribution of the annual maximum (or minimum) values of meteorological elements, Quart. J. R. Meteorol. Soc., 81, 158 – 171.

Lanza, L. G., Vuerich, E., and Gnecco, I.: Analysis of highly accurate rain intensity measurements from a field test site, Adv. Geosci., 25, 37–44, https://doi.org/10.5194/adgeo-25-37-2010, 2010.

Lazoglou, Georgia and Anagnostopoulou, Chr and Tolika, K and Kolyva-Machera, Fotini. (2018). A review of statistical methods to analyze extreme precipitation and temperature events in the Mediterranean region. Theoretical and Applied Climatology. 10.1007/s00704-018-2467-8.

Lutz, J.; Grinde, L.; Dyrrdal, A.V. Estimating Rainfall Design Values for the City of Oslo, Norway—Comparison of Methods and Quantification of Uncertainty. Water 2020, 12, 1735. https://doi.org/10.3390/w120617350

Marra F., Morin E., Use of radar QPE for the derivation of Intensity–Duration–Frequency curves in a range of climatic regimes, Journal of Hydrology, Volume 531, Part 2, 2015, Pages 427-440, ISSN 0022-1694, https://doi.org/10.1016/j.jhydrol.2015.08.064.

Marra, F., Morin, E., Peleg, N., Mei, Y., and Anagnostou, E. N.: Intensity–duration–frequency curves from remote sensing rainfall estimates: comparing satellite and weather radar over the eastern Mediterranean, Hydrol. Earth Syst. Sci., 21, 2389–2404, https://doi.org/10.5194/hess-21-2389-2017, 2017.

F. Marra, E. I. Nikolopoulos, E. N. Anagnostou, A. Bárdossy, E. Morin, Precipitation frequency analysis from remotely sensed datasets: A focused review, Journal of Hydrology, Volume 574, 2019, Pages 699-705, ISSN 0022-1694, https://doi.org/10.1016/j.jhydrol.2019.04.081

Marra, F. and Armon, M. and Morin, E., Coastal and orographic effects on extreme precipitation revealed by weather radar observations,Hydrology and Earth System Sciences,26, 2022, 5,1439-1458,https://hess.copernicus.org/articles/26/1439/2022/, doi: 10.5194/hess-26-1439-2022

Mazzoglio, P. and Butera, I. and Alvioli, M. and Claps, P., The role of morphology in the spatial distribution of short-duration rainfall extremes in Italy,Hydrology and Earth System Sciences, 26, 2022, 6, pp. 1659-1672, https://hess.copernicus.org/articles/26/1659/2022/, doi: 10.5194/hess-26-1659-2022

Moisseev D., Keränen R., Puhakka P., Salmivaara J., Leskinen M. 2010: Analysis of dual-polarization antenna performance and its effect on QPE, 6th European Conference on Radar in Meteorology and Hydrology, Sibiu, Romania;

Naimi, B., Skidmore, A.K, Groen, T.A., Hamm, N.A.S. 2011. Spatial autocorrelation in predictors reduces the impact of positional uncertainty in occurrence data on species distribution modelling, Journal of biogeography. 38: 1497-1509.

Jonas Olsson, Anita Verpe Dyrrdal, Erika Médus, Johan Södling, Svetlana Aniskeviča, Karsten Arnbjerg-Nielsen, Eirik Førland, Viktorija Mačiulytė, Antti Mäkelä, Piia Post, Søren Liedke Thorndahl, Lennart Wern; Sub-daily rainfall extremes in the Nordic–Baltic region. Hydrology Research 1 June 2022; 53 (6): 807–824. doi: https://doi.org/10.2166/nh.2022.119

Overeem, Aart and Buishand, Adri and Holleman, Iwan. (2008). Rainfall depth-duration-frequency curves and their uncertainties. Journal of Hydrology. 348. 124-134. 10.1016/j.jhydrol.2007.09.044.

Overeem, A., A. Buishand, and I. Holleman (2009a), Extreme rainfall analysis and estimation of depth-duration-frequency curves using weather radar, Water Resour. Res., 45, W10424, doi:10.1029/2009WR007869.

Overeem, A., I. Holleman, and A. Buishand (2009b), Derivation of a 10 year radar-based climatology of rainfall, J. Appl. Meteorol. Climatol., 48, 1448–1463, doi:10.1175/2009JAMC1954.1.

Overeem, A., T. A. Buishand, I. Holleman, and R. Uijlenhoet (2010), Extreme value modeling of areal rainfall from weather radar, Water Resour. Res., 46, W09514, doi:10.1029/2009WR008517.

L. Panziera, M. Gabella, U. Germann and O. Martius, A 12-year radar-based climatology of daily and sub-daily extreme precipitation over the Swiss Alps, International Journal of Climatology, 38, 10, (3749-3769), (2018).

Papalexiou, S.M. and Koutsoyiannis, D., 2013. Battle of extreme value distributions: A global survey on extreme daily rainfall. Water Resources Research, 49, 187–201. doi:10.1029/2012WR012557

Paulitsch, H., Teschl, F., and Randeu, W. L.: Dual-polarization C-band weather radar algorithms for rain rate estimation and hydrometeor classification in an alpine region, Adv. Geosci., 20, 3-8, https://doi.org/10.5194/adgeo-20-3-2009, 2009.

Pavan, V., Antolini, G., Barbiero, R. et al. High resolution climate precipitation analysis for north-central Italy, 1961–2015. Clim Dyn 52, 3435–3453 (2019) doi:10.1007/s00382-018-4337-6 ~~Peleg, Nadav and Marra, Francesco and Fatichi, Simone and Paschalis, Athanasios and Molnar, Peter and Burlando, Paolo. (2016). Spatial variability of extreme rainfall at radar subpixel scale. Journal of Hydrology. 10.1016/j.jhydrol.2016.05.033.~~

Ragulina, Galina and Reitan, Trond. (2017). Generalized extreme value shape parameter and its nature for extreme precipitation using long time series and the Bayesian approach. Hydrological Sciences Journal. 62. 1-17. 10.1080/02626667.2016.1260134.

Reimel, K. J., and Kumjian, M., 2021). Evaluation of KDP Estimation Algorithm Performance in Rain Using a Known-Truth Framework, Journal of Atmospheric and Oceanic Technology, 38(3), 587-605. Retrieved Jun 15, 2021, from https://journals.ametsoc.org/view/journals/atot/38/3/JTECH-D-20-0060.1.xml

Ryzhkov, A.V., Schuur, T.J., Burgess, D.W., Heinselman, P.L., Giangrande, S.E. and Zrnic, D.S. (2005). The Joint Polarization Experiment: Polarimetric rainfall measurements and hydrometeor classification. Bulletin of the American Meteorological Society, 86(6), pp.809-824.

Ryzhkov, A.V., Kumjian, M.R., Ganson, S.M. and Zhang, P. (2013). Polarimetric radar characteristics of melting hail. Part II: Practical implications. Journal of Applied Meteorology and Climatology, 52(12), pp.2871-2886.

Schroeer, K., Kirchengast, G., and O. S. (2018). Strong dependence of extreme convective precipitation intensities on gauge network density. Geophysical Research Letters, 45, 8253– 8263. https://doi.org/10.1029/2018GL077994

Tammets, T., and Jaagus, J. (2013). Climatology of precipitation extremes in Estonia using the method of moving precipitation totals. Theoretical and Applied Climatology, 111(3), 623-639.

A. Viglione, F. Laio, P. Claps A comparison of homogeneity tests for regional frequency analysis, Water Resour. Res., 43 (2007), p. W03428

Voormansik, T., Cremonini, R., Post, P., and Moisseev, D.: Evaluation of the dual-polarization weather radar quantitative precipitation estimation using long-term datasets, Hydrol. Earth Syst. Sci., 25, 1245–1258, ~~, 2021.~~ https://doi.org/10.5194/hess-25-1245-2021, 2021a

Voormansik, T., ~~Müürsepp~~Műűrsepp, T., and Post, P.: Climatology of Convective Storms in Estonia from Radar Data and Severe Convective Environments, Remote Sens., 13(11), 2178, ~~, 2021.~~ https://doi.org/10.3390/rs13112178, 2021b

Vuerich, E., Monesi, C., Lanza, L., Stagi, L., Lanzinger, E.: WMO Field Intercomparison of Rainfall Intensity Gauges, Vigna di Valle, Italy, October 2007-April 2009, WMO/TD- No. 1504; IOM Report- No. 99, 2009.

Gianfranco Vulpiani, Mario Montopoli, Luca Delli Passeri, Antonio G. Gioia, Pietro Giordano, and Frank S. Marzano, 2012: On the Use of Dual-Polarized C-Band Radar for Operational Rainfall Retrieval in Mountainous Areas. J. Appl. Meteor. Climatol., 51, 405-425, doi: 10.1175/JAMC-D-10-05024.1.

Wang, Y. and V. Chandrasekar. (2009). Algorithm for Estimation of the Specific Differential Phase. J. Atmos. Oceanic Technol., 26, 2565–2578, https://doi.org/10.1175/2009JTECHA1358.1

Wilks, Daniel S. Statistical Methods in the Atmospheric Sciences. 3rd ed. Oxford ; Waltham, MA: Academic Press, 2011.